Relationship between the two-component system 1-Br-adamantane + 1-Cl-adamantane and the high-pressure properties of the pure components

María Barrio [a], Rafael Levit [a], Pol Lloveras [a, *], Araceli Aznar [a], Philippe Negrier [b], Denise Mondieig [b], Josep-Lluís Tamarit [a]

[a] Grup de Caracterització de Materials, Departament de Física, EEBE and Barcelona Research Center in Multiscale Science and Engineering, Universitat Politècnica de Catalunya, Eduard Maristany, 10-14, 08019 Barcelona, Catalonia, Spain

[b] LOMA, UMR 5798, CNRS, Université de Bordeaux, F-33400 Talence, France

(*) Corresponding author: pol.lloveras@upc.edu

Phone: +34 934010824

Keywords: High pressure, polymorphism, two-component system

Abstract

The temperature-composition phase diagram of the two-component system 1-Br-adamantane and 1-Cl-adamantane has been determined by means of thermal analysis techniques and X-ray powder diffraction from the low-temperature phase to the liquid state. The crossed isopolymorphism formalism has been applied to the two-component system to infer the normal pressure properties of the orthorhombic metastable phase of 1-Cl-adamantane at normal pressure. The experimental pressure-temperature phase diagrams for the involved compounds are related to the two-phase equilibria determined at normal pressure and inferences about the monotropic behavior of the aforementioned orthorhombic phase are discussed.

1. Introduction

One of the major challenges of the solid-state field is not only the understanding of the structural and thermodynamic factors ruling the polymorphism but also the ability to predict the crystalline phases of molecular materials for both large technological systems as well as for fundamental thermodynamics. The classical understanding of polymorphism has been commonly restricted to the phase stability of a material as a function of temperature, but strictly speaking stability should be accounted within the pressure-temperature space obtained from the classical Gibbs thermodynamics. Many of the physical and chemical properties for simple or complex systems are known at or near atmospheric pressure while effects of the high pressures remain still unexplored. In particular, although high-pressure studies have become of great interest for metal, semiconductor or, in general, mineral systems, molecular compounds with increasing complexity remain to be understood under pressure and in this particular field, polymorphism concept refers usually to the ability of a substance to adopt more than one crystalline form in the solid state without any comment about the pressure variable.

Even more, the field of phase diagrams involving at least two chemical species, the temperature-composition (*T*-*X*) phase diagrams, is generally decoupled from the field of the polymorphic behavior at high pressure. Nevertheless, thermodynamics imposes an univocal relation between the controlled pressure and temperature conditions at which a polymorph should exist and the physical properties derived at normal pressure and, hence, the properties that can be extracted from a temperature-composition phase diagram [1-15]. The other way around also holds, properties derived for stable or metastable phases emerging in the temperature-composition phase diagrams can provide information about the nature of high-pressure phases even when they do not exist as stable phases at normal pressure.

This work concerns the experimental determination of the pressure-temperature phase diagrams of 1-Br-adamantane and 1-Cl-adamantane and their two-component system, as well as the connection between these rarely combined fields.

The adamantane molecule ($C_{10}H_{16}$) is formed by a 10-carbon cage made of four cyclohexane rings in chair conformation. The adamantane compound is known to display a wide temperature range of the plastic phase (from 208 to 543 K) [16] due to the molecular spherical shape (T_d symmetry). The plastic phases are orientationally disordered (OD) phases in which the molecules perform reorientations more or less freely among a set of distinguishable number of equilibrium orientations displaying usually a high space-group symmetry lattice (hexagonal or cubic). By the replacement of one or more hydrogen atoms in the adamantane molecule by a substituent X (X = OH, F, Cl, I, etc.) the symmetry of the molecule, and thus intermolecular interactions and steric effects change. By a single substitution on a tertiary carbon, the series of 1-X-adamanane, with C_{3v} point-group symmetry, is derived.

The phase behavior of the 1-X-adamantane compounds varies according to the substituent. Most of these derivatives show up an OD phase prior to melting, for example, 1-chloroadamantane (1-ClA, hereinafter), 1-bromoadamantane (1-BrA) and 1-cyanoadamantane [17-24]. These compounds may also have one or several solid−solid transitions, as for 1-BrA, which exhibits three solid-solid phase transitions, one of them being at very low temperature (31.0 K), which will not be considered in this work. **Table 1** shows the thermodynamic properties of 1-ClA and 1-BrA. As for 1-ClA, the low-

temperature monoclinic (space group $P2_1/c$) phase transforms to the OD phase (space group Fm-3m) at ca. 249 K which melts at 439 K [25]. As for 1-BrA, the lowest temperature phase, isostructural to the monoclinic $P2_1/c$ phase of 1-ClA [26], transforms to an intermediate orthorhombic (space group Pmcn) phase at ca. 311 K [27]. On further heating, such phase transforms to the high-temperature OD (Fm-3m) phase [28] which melts at 392 K.

Concerning 2-X-adamantane (with C_{2v} molecular symmetry) obtained from the substitution through at a secondary carbon, much less reactive, the rich polymorphic behavior has recently been revealed for X = Cl, Br and O [17,18,29].

Table 1. Transition temperatures T and enthalpy (ΔH) and entropy changes (ΔS) derived from DSC calorimetric measurements, volume changes determined from X-ray powder diffraction measurements (Δv^{XR}), slope of the pressure-temperature two-phase equilibria derived from the experimental pressure-temperature phase diagram $(dT/dP)^{exp}$ and from the application of the Clapeyron equation $(dT/dP)^{C}$. M refers to the low-temperature monoclinic ($P2_1/c$) phase, O to the intermediate orthorhombic phase (Pmcn) and FCC for the face-centered cubic (Fm-3m) orientationally disordered (OD) phase. The superscript S and m refer to stable and metastable phases, respectively. Numbers in italic refer to metastable phases.

1-Br-adamantane					
Property	$M^S \rightarrow O^S$	$M^S \rightarrow FCC^m$	$O^S \rightarrow FCC^S$	$FCC^S \rightarrow L^S$	Ref.
T / K	282.2 ± 0.1		309.9 ± 0.1	391.8 ± 0.2	[30]
	279		310.5	396.5	[32]
	282.6 ± 1.0	*308.2 ± 1.5*[£]	310.8 ± 1.0	392.0 ± 1.5	This work
ΔH / kJ mol^{-1}	1.387± 0.012		7.51 ± 0.15	3.97 ± 0.80	[30]
	0.88		6.93	3.83	[32]
	1.26 ± 0.06	*7.84 ± 0.55*[£]	6.69 ± 0.35	3.25 ± 0.20	This work
ΔS / J mol^{-1} K^{-1}	4.92 ± 0.04		24.2 ± 0.5	10.1 ± 0.2	[30]
	4.46 ± 0.22	*25.43 ± 2.0*[£]	21.54 ± 1.1	8.27 ± 0.51	This work
Δv^{XR} (P = 0.1MPa) / cm^3 mol^{-1}	1.26 ± 0.10	*9.70 ± 0.16*	8.56 ± 0.03	-	This work
$(dT/dP)^{C}$ / K MPa^{-1}	0.281 ± 0.036	*0.381 ± 0.040*	0.397 ± 0.022	-	This work
$(dT/dP)^{exp}$ / K MPa^{-1}	0.251 ± 0.015		0.336 ± 0.006	0.268 ± 0.019	This work
1-Cl-adamantane					
Property	$M^S \rightarrow O^m$	$M^S \rightarrow FCC^S$	$O^m \rightarrow FCC^s$	$FCC^S \rightarrow L^S$	Ref.
T / K		248.6 ± 0.1		439.7 ± 0.1	[31]
		246		442.5	[32]
	269.6 ± 1.5[£]	249.5 ± 1.0	*246.8 ± 1.5*[£]	438.6 ± 1.5	This work
ΔH / kJ mol^{-1}		4.30 ± 0.02		5.53 ± 0.01	[31]
		6.01		4.87	[32]
	0.76 ± 0.08[£]	5.96 ± 0.30	*5.44 ± 0.56*[£]	4.22 ± 0.25	This work

ΔS / J mol^{-1} K^{-1}		17.3 ± 0.01		17.3 ± 0.1	[31]
	2.83 ± 0.30 [£]	23.88 ±1.20	*22.06 ± 2.27*[£]	9.61 ± 0.57	This work
Δv^{XR} **(*P* = 0.1MPa)** / cm^3 mol^{-1}	*2.12 ± 0.30*[#]	7.95 ± 0.51	*6.09 ± 0.91*[#]	-	This work
$(dT/dP)^{C}$ / K MPa^{-1}	*0.71 ± 0.21*	0.33 ± 0.04	*0.28 ± 0.08*	-	This work
$(dT/dP)^{exp}$ / K MPa^{-1}	-	0.270 ± 0.005	-	-	This work

[£] Extrapolated from the two-component system assessment.

[#] From the X-ray diffraction measurements as a function of the composition.

2. Experimental

2.1. Materials

1-BrA and 1-ClA were purchased from Aldrich with purity of 99% and 98% (as summarized in the **Supplementary Material** in **Table S1**), respectively, and used as received since the measured phase transition and melting points agreed well with those previously reported [30,31]. Two-component mixtures were prepared from the melt of the materials in the selected proportions and fast cooling to room temperature.

2.2 Thermal analysis

Differential Thermal Analysis (DTA) at normal pressure. Thermal properties of the phase transitions (temperatures and enthalpy changes) were determined by means of a Q100 from TA Instruments using heating and cooling scanning rates of 2 K min^{-1}. Sample masses about 10 mg were weighted using a microbalance sensitive to 0.01 mg and were hermetically sealed into aluminum crucibles under a controlled N_2 atmosphere.

High-Pressure (HP) Differential Thermal Analysis. Measurements were carried out at 2 K min^{-1} heating rate by means of an in-house built high-pressure differential thermal analyzer similar to Würflinger's apparatus [33]. Temperature and pressure ranges were between 200 and 450 K and 0 and 300 MPa, respectively. Samples were mixed with inert perfluorinated liquid (Galden, Bioblock Scientifics, France) before the high-pressure Sn pans were hermetically closed to make sure that in-pan volumes were free of air. DTA runs at normal pressure using the Q100 under ordinary conditions were performed prior to the high-pressure differential thermal analyses in order to verify that perfluorinated liquid was chemically inactive when mixed with both compounds.

2.3. X-ray powder diffraction

High-resolution X-ray powder diffraction measurements using the Debye–Scherrer geometry and transmission mode were performed with a horizontally mounted INEL cylindrical position-sensitive detector (CPS-120) made of 4096 channels (0.029^o 2θ-angular step) [34]. Monochromatic Cu-Kα1 (λ = 1.54056 Å) radiation was selected by means of an asymmetrically focusing incident-beam curved germanium monochromator. The generator power was set to 40 kV and 25 mA. Measurements as a function of

temperature were performed using a liquid nitrogen 700 series Cryostream Cooler from Oxford Cryosystems.
External calibration was performed by means of cubic phase $Na_2Ca_3Al_2F_4$. The peak positions were determined by pseudo-Voigt fittings. Powder samples were introduced into 0.5 mm diameter Lindemann capillaries which were rotated around their axes during data collection to improve averaging of the crystallites. The acquisition times were of at least 120 min for the low-temperature ordered phases and 60 min for the high-temperature OD FCC phases. Stabilization times of at least 10 min at each temperature before the data acquisition were preset.
Indexing of the X-ray powder diffraction patterns, structure solutions, and Pawley and Rietveld refinements were performed using Materials Studio Program [35].

3. Results

3.1 Characterization of materials

3.1.1. 1-Br-adamantane ($C_{10}H_{15}Br$)

The crystal structure of the low-temperature phase determined by means of a single crystal study as monoclinic (M) space group $P2_1/c$ [26] with Z = 4 was checked by X-ray powder diffraction. At 282 K it transforms to an orthorhombic (O) phase, the details of this structure will be given in a later work. At 309.9 K such phase transforms to the orientationally disordered (OD) face-centered cubic (FCC) phase, which remains up to the melting point at ca. 392 K.
X-ray powder diffraction experiments as a function of temperature were carried out from 90 K up to the liquid state. Lattice parameters of the low-temperature M and O ordered phases were refined by applying Rietveld profile refinements by means of the Materials Studio Program [35] on the basis of the proposed structure for the M structure [26] and by using a rigid molecule approach for the O phase. The experimental and calculated profiles together with the difference between them for both phases are shown in in the **Supplementary Material** in **Fig. S1**. The M lattice parameters agree quite well with those previously published [26]. At 210.0 K they have been determined to be a = 10.1125(5) Å, b = 6.8485(3) Å, c = 13.2388(6) Å and β = 90.246(3)°, rendering V/Z = 229.21(2) Å^3. As for the O phase the space group was determined as Pmcn and lattice parameters at 290 K were found to be a = 10.119(7) Å, b = 6.8936(5) Å and c = 13.6043(8) Å, rendering V/Z = 237.25 (2) Å^3.

The refined lattice parameters were fitted as a function of the temperature using standard least squares methods for each parameter. The agreement between the calculated and experimental values has been accounted by the reliability factor, defined as $R = \sum (y_o - y_c)^2 / y_c^2$, where y_o and y_c stand for the measured and calculated lattice parameters, respectively. **Table 2** gathers the coefficients of the polynomial equations and **Fig. 1** depicts both experimental values and polynomials for the monoclinic phase.

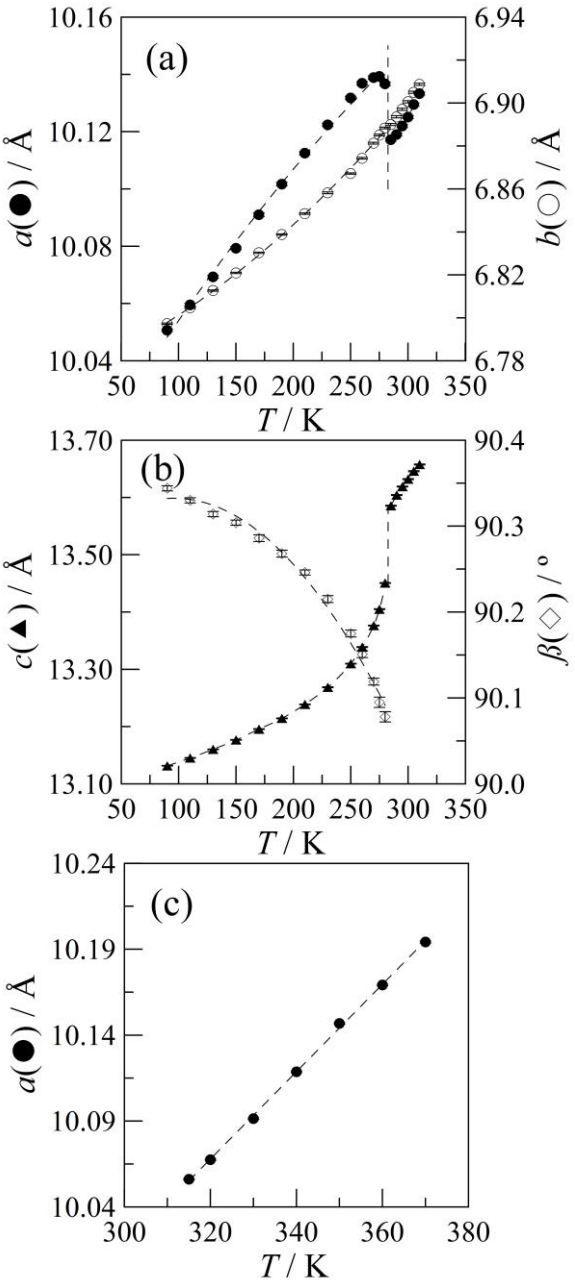

Fig. 1. Lattice parameters of 1-BrA for the low-temperature monoclinic and orthorhombic (a and b) and for OD FCC (c) phases as a function of temperature.

Through HP DTA experiments the M-O, O-FCC and FCC-L two-phase equilibria as a function of pressure were determined. The so-obtained pressure-temperature phase diagram is displayed in **Fig. 2(a)** (for the numerical values see **Table S2** in the **Supplementary**

Material). Although the temperature range of the OD phase usually increases with pressure [36-38], the OD phase for 1-BrA has an opposite behavior.

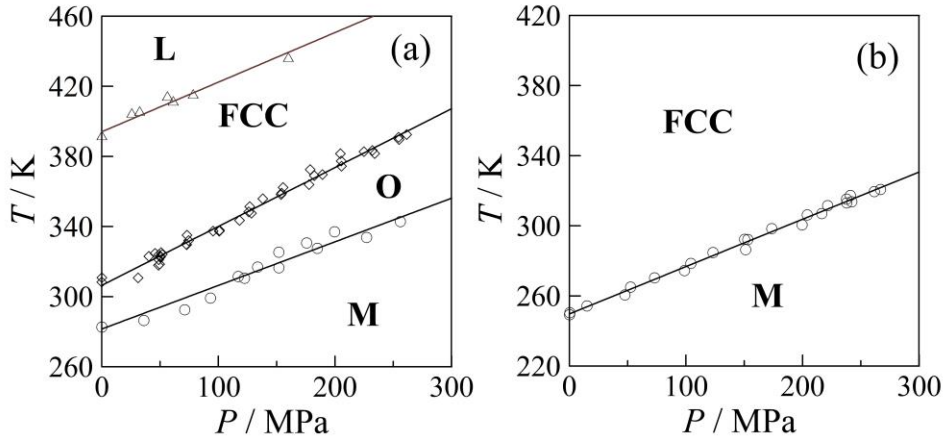

Fig. 2. Pressure−temperature phase diagram of 1-BrA (a) and 1-ClA (b) obtained from high-pressure differential thermal analysis.

3.1.2. 1-Cl-adamantane ($C_{10}H_{15}Cl$)

The polymorphism of 1-ClA is simpler than that of 1-BrA. It reveals the existence of a monoclinic low-temperature phase, with a space group $P2_1/c$, so isostructural to the low-temperature monoclinic phase of 1-BrA as revealed by Foulon *et al*. [25]. The authors also concluded that the size of the molecule, i.e., of the halogen substituent, controls the lattice dimension and, as a consequence, the lattice parameters. At 249.5 K the monoclinic phase transforms to an OD FCC phase which melts at 438.6 K. The OD FCC phase was also found to be isostructural (Fm-3m) to the high-temperature OD phase of 1-BrA. The result of the Rietveld refinement of the monoclinic phase of 1-ClA is shown in the **Supplementary Material** in **Fig. S2**. Lattice parameters were fitted as a function of the temperature and they are displayed in **Fig. 3**. **Table 2** gathers the coefficients of the polynomial equations for the variation of the lattice parameters as a function of temperature.

The pressure-temperature phase diagram for the M-FCC equilibrium [**Fig. 2(b)**] was determined by means of HP DTA. As for the melting of 1-ClA, the temperature domain was beyond the available temperature range of the experimental device.

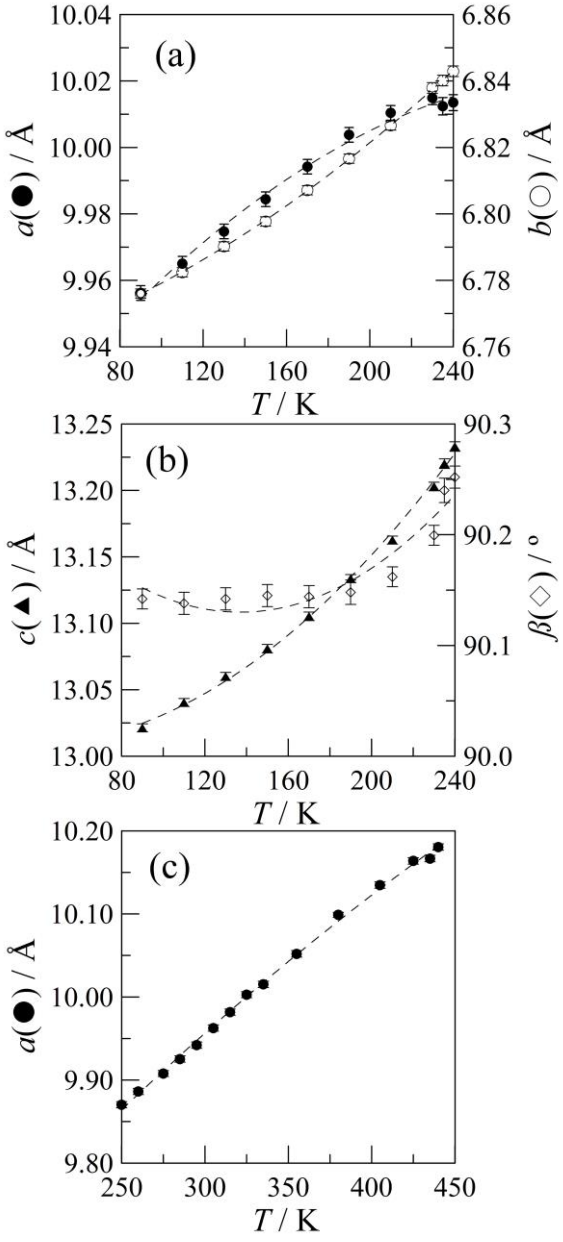

Fig. 3. Lattice parameters of 1-ClA for the low-temperature monoclinic (a and b) and for OD FCC (c) phases as a function of temperature.

Table 2. Polynomial equations $p=p_o+p_1T+p_2T^2$ *(T in K and p in Å or in* ^{o} *for* β *parameter*) to which the lattice parameters were fitted as a function of temperature. R is the reliability factor.

Phase	**Temperature range (K)**	**Parameter**	p_o	$p_1 \cdot 10^3$	$p_2 \cdot 10^5$	$R \cdot 10^5$

1-Br-adamantane

M ($P2_1/c$)	90-280 K	*a*	9.991(8)	0.68(9)	-0.05(2)	8.2
		b	6.773(3)	2.01 (4)	0.07(9)	6.3
		c	13.238(3)	-1.79(6)	0.86 (2)	4.0
		β	90.27(3)	1.36(3)	-0.71(2)	0.2
O (Pmcn)	285-310 K	*a*	10.914(18)	-5.97(1)	1.11(2)	0.9
		b	6.676(4)	0.75(1)		0.008
		c	10.314(5)	19.4(4)	-2.79(6)	0.5
FCC	315-370 K	*a*	9.255(11)	2.54(3)		0.01

1-Cl-adamantane

M ($P2_1/c$)	90-240 K	*a*	9.888(9)	0.86(11)	-0.14(3)	0.03
		b	6.754(1)	0.17(2)	0.08(4)	0.001
		c	13.010(17)	-0.28(22)	0.49 (6)	0.02
		$\beta^{(\&)}$	89.78(15)	8.18(31)	-6(2)	0.007
FCC	250-440 K	*a*	9.308(5)	2.52(3)	-0.12(4)	14

$^{(\&)}$For the β angle of M phase of 1-ClA the polynomial is third-order, with third-order coefficient $1.4(4)\cdot10^{-7}$.

3.2. Two-component system

3.2.1 Thermal Analysis

Solid-solid transition and melting temperatures together with the associated enthalpy changes were determined by means of DTA at normal pressure. The resulting temperature-composition phase diagram is represented by **Fig. 4**. The two-component system displays a metatectoid three-phase equilibrium at 274.5 ± 1.0 K sharing M (X_M = 0.585), O (X_O = 0.60) and FCC (X_{FCC} = 0.71) phases. It clearly appears that the M and the FCC phases for both components form continuous solid solutions (see crystallographic characterization).

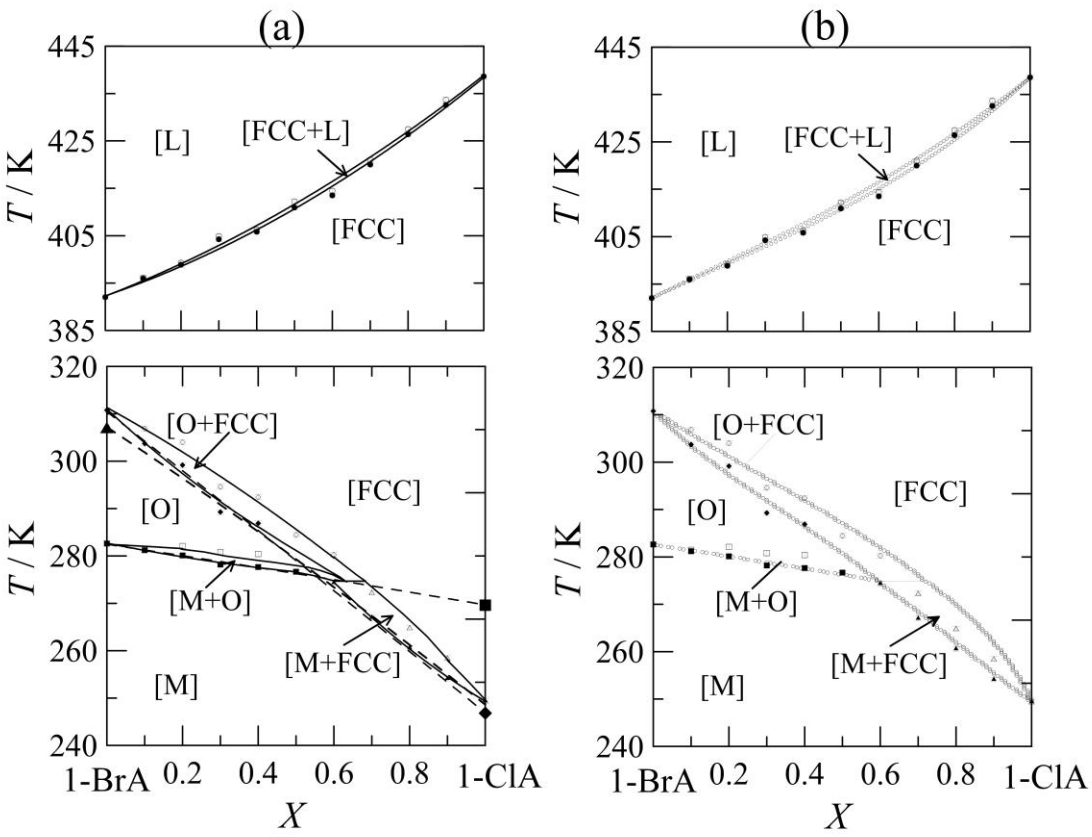

Fig. 4. 1-BrA + 1-ClA phase diagram at normal pressure. Symbols correspond to experimental data. Empty squares (□) denote $T^{[M+O]\text{-}FCC}$. Filled squares (■) denote $T^{M\text{-}[M+O]}$. Empty triangles (Δ) denote $T^{[M+FCC]\text{-}FCC}$. Filled triangles (▲) denote $T^{M\text{-}[M+FCC]}$. Empty diamonds (◊) denote $T^{[O+FCC]\text{-}FCC}$. Filled diamonds (♦) denote $T^{O\text{-}[O+FCC]}$. In panel (a), the metastable temperatures $T^{M\text{-}FCC}$ (large ▲) for pure 1-BrA and $T^{M\text{-}O}$ (large ■) and $T^{O\text{-}FCC}$ (large ♦) for pure 1-ClA are shown. Lines in (a) are fits to the data whereas lines in (b) correspond to the calculated phase diagram by means of the common tangent construction method as described in Sec. 3.2.3.

The enthalpy changes involved in the solid-solid transitions and the melting process derived from the thermal measurements are depicted in **Fig. 5**.

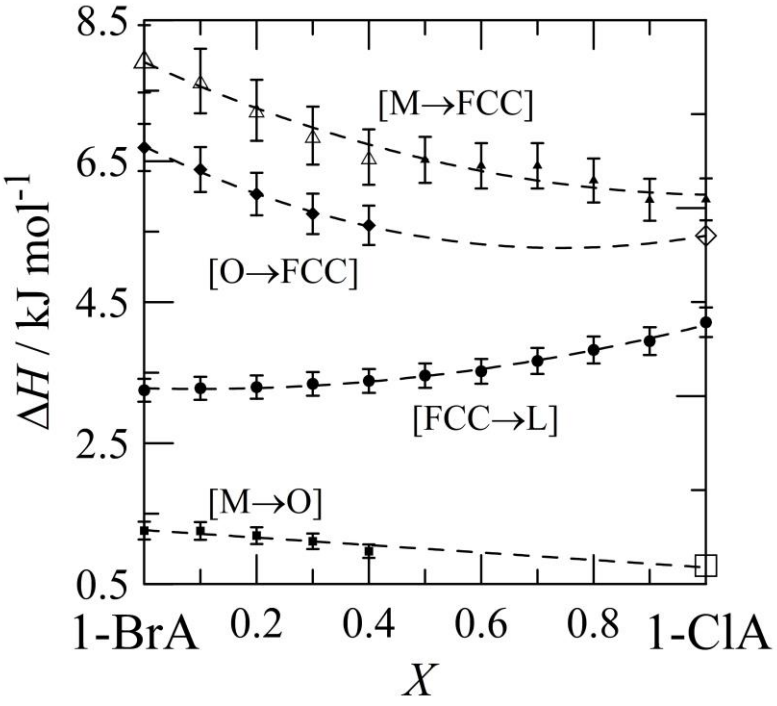

Fig. 5. Experimental (full symbols) enthalpies of solid-solid transitions and melting of the FCC phase as a function of the mole fraction. Empty symbols at $X = 0$ and $X = 1$ correspond to the extrapolated values for transitions involving at least one metastable phase, whereas empty triangles are calculated according to eq. (6) (see text).

3.2.2. Crystallographic characterization

Monoclinic mixed crystals. The monoclinic phases for both 1-BrA and 1-ClA compounds have been found isostructural ($P2_1/c$) and the continuous formation of mixed crystals, as revealed by the thermal analysis (**Figs 4** and **5**), as a function of composition has been verified at 225 K. **Fig. 6** shows the continuous variation of the monoclinic lattice parameters as a function of mole fraction.

Orthorhombic mixed crystals. The miscibility for the orthorhombic phase is truncated by the emergence of the [O+FCC] two-phase equilibrium (see **Fig. 4**). Lattice parameters were determined at 290 K (see **Fig. 7**) for the composition range comprised between $X = 0$ and $X = 0.4$.

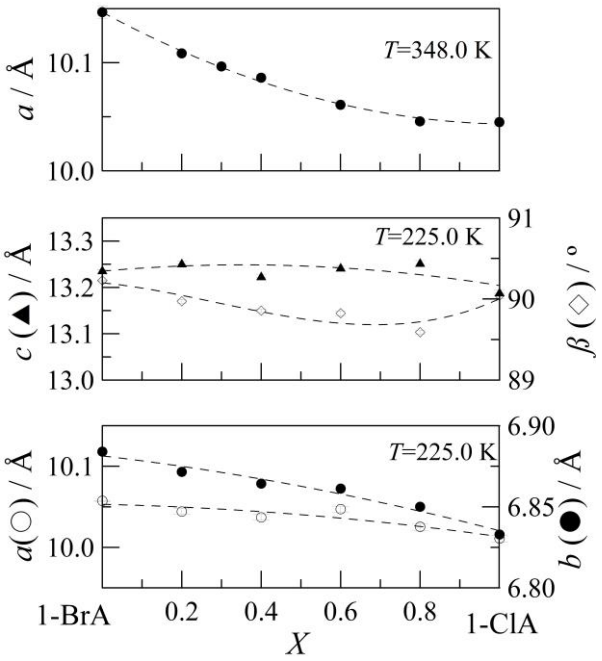

Fig. 6. Monoclinic (lower panels) and FCC (top panel) lattice parameters at 225 and 348 K, respectively, as a function of mole fraction.

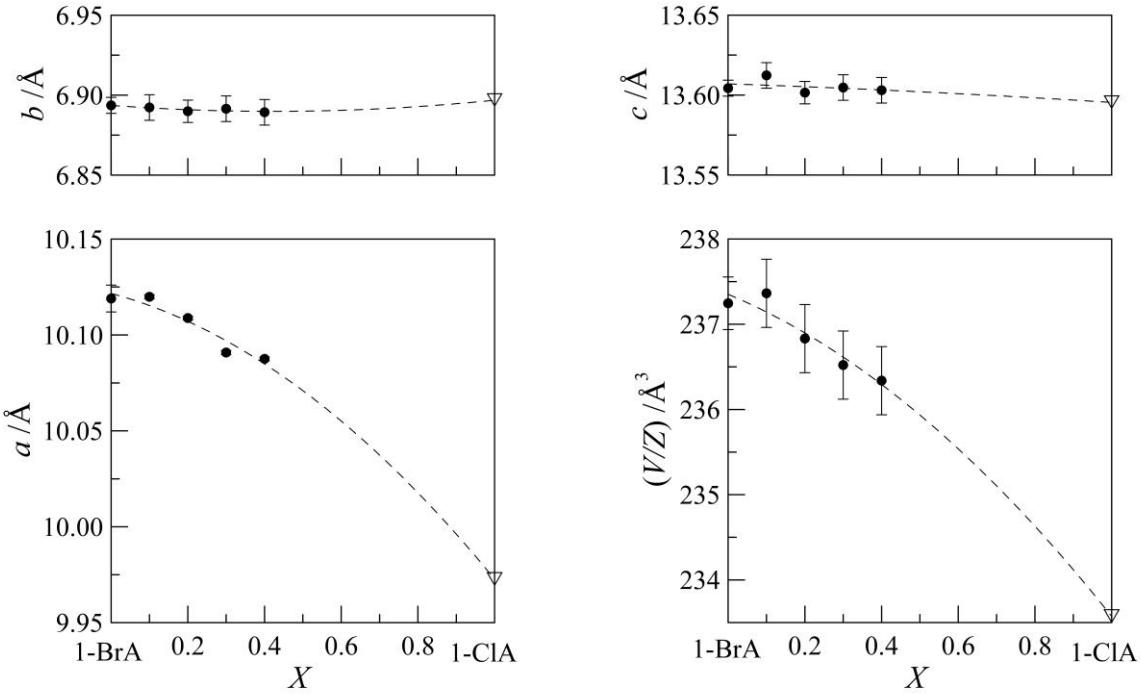

Fig. 7. Orthorhombic lattice parameters and volume per molecule at 290 K as a function of mole fraction. The empty symbols correspond to the parameters values of the metastable orthorhombic phase of 1-ClA compound.

Face-centered cubic mixed crystals. To account for the existence of complete miscibility of the FCC phases, X-ray powder diffraction was conducted at 348 K. Lattice parameters for such a domain are depicted in **Fig. 6** (top panel). The continuity of the variation of the lattice parameter together with the *T*-X loop found through thermal analysis ensure the isomorphism relationship between the FCC phases of the pure components.

3.2.3. Thermodynamic assessment

The thermodynamic analysis has been based on the crossed isopolymorphism [3,6,7,11,13] and the Equal-Gibbs-Curve concepts [39]. We briefly describe both concepts for the sake of completeness.

The crossed isopolymorphism is sketched in **Fig. 8** for this case. The form M is stable for component A and for component B, while the form O is only stable for component A (O is metastable for B), FCC being stable for both components. The "stable" phase diagram can be looked upon as the stable result of three, each other crossing, two-phase loops. The three crossing loops imply a stable three-phase equilibrium (M+O+FCC), which, in the case of **Fig. 8**, is a metatectoid, as for the phase diagram (see **Fig. 4**) of the present study.

Any phase ϕ we consider in which (1 - X) mole of component A mixes with X mole of component B, is characterized by its own Gibbs function

$$G^{\phi}(T,X) = (1-X)\mu_A^{*,\phi}(T) + X\mu_B^{*,\phi}(T) + RT\left[X\ln(X) + (1-X)\ln(1-X)\right] + G^{E,\phi}(T,X) \qquad (1)$$

where T stands for the temperature, R the gas constant, $\mu_k^{*,\phi}(T)$, k = A, B denote the molar Gibbs energies of the components, and $G^{E,\phi}(T,X)$ the excess Gibbs energy which accounts for the deviation of the mixture in the ϕ phase from ideal-mixing behavior produced by interactions between molecular species A and B with regard to the interactions between molecules of the same species (A-A and B-B).

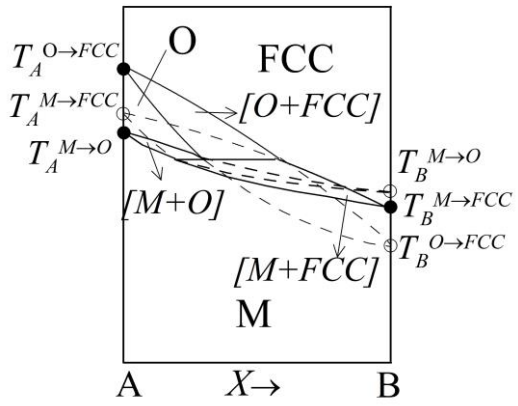

Fig. 8. Solid and dashed curves represent stable and metastable behavior, respectively. Filled and empty circles represent the stable and metastable transition points, respectively.

To determine the two-phase equilibrium region between two phases (ϕ and γ), i.e., the concentration limits of the loop for the coexisting phases, the well-known equilibrium rule minimizing the Gibbs energy of the mixed crystal $A_{1-X}B_X$ at each temperature, which consists on the common tangent to both Gibbs energies characterizing the phases of the corresponding equilibrium, $G^{\phi}(T,X)$ and $G^{\gamma}(T,X)$, must be determined. For this task, the molar Gibbs energies of the pure compounds A and B as well as the excess properties for

each phase are required. Because of the lack of data on $\mu_k^{*,\phi}$, k = A, B, the simplified treatment of the equal-Gibbs curve (EGC) method will be used [39].

To do so, the difference between the Gibbs energies of phases ϕ and γ is written as

$$\Delta_\phi^\gamma \mathrm{G(T, X)} = \mathrm{G}^\gamma(T,X) - G^\phi(T,X) = (1-X)\Delta_\phi^\gamma \mu_A^*(T) + X\Delta_\phi^\gamma \mu_B^*(T) + \Delta_\phi^\gamma G^E(T,X) \quad (2)$$

where $\Delta_\phi^\gamma \mu_k^*(T)$ is $\mu_k^{*,\gamma} - \mu_k^{*,\phi}$ (k = A, B) and $\Delta_\phi^\gamma G^E(T,X)$ is the excess Gibbs energy difference between the considered phases, i.e., $G^{E,\gamma}(T,X) - G^{E,\phi}(T,X)$.

The existence of equilibrium at a given temperature implies necessarily that the Gibbs functions of the ϕ and γ phases intersect, and thus the locus of the points of intersection in the *TX* plane (the EGC) will be the result of equation:

$$\Delta_\phi^\gamma \mathrm{G}(T_{EGC}, X) = 0 \quad (3)$$

$\Delta\mu_k^*(T)$ can be approximately written as $\Delta_\phi^\gamma \mathrm{S}_k^*(T_k^{\phi\to\gamma} - T)$, neglecting the heat capacities differences between both phases, being $T_k^{\phi\to\gamma}$ the temperature of the $\phi\to\gamma$ transition for the component *k*, the EGC temperature can be deduced from eq. (3) as:

$$T_{\mathrm{EGC}} = \frac{(1-X)\Delta_\phi^\gamma H_A^* + X\Delta_\phi^\gamma H_B^*}{(1-X)\Delta_\phi^\gamma S_A^* + X\Delta_\phi^\gamma S_B^*} + \frac{\Delta_\phi^\gamma G_{EGC}^E(X)}{(1-X)\Delta_\phi^\gamma S_A^* + X\Delta_\phi^\gamma S_B^*} \quad (4)$$

where $\Delta_\phi^\gamma H_k^*$ and $\Delta_\phi^\gamma S_k^*$ are the enthalpy and entropy changes of the $\phi \to \gamma$ transition for the component *k*. The first term of the right side of eq. (4) represents the EGC temperature for the [ϕ+γ] equilibrium when $\Delta_\phi^\gamma G^E(T,X) = 0$ and is only pure component-dependent and thus can be obtained from pure component data. Nevertheless, some of the metastable properties as heats of transition and transition points must be obtained in an indirect manner when a crossed-isomorphism is considered.

A first estimation of the EGC curve can be done from the experimental data of the two-phase equilibrium. By an iterative procedure performed by means of the LIQFIT program [40] based on Oonk's method enables one to obtain the values of the excess Gibbs energy differences at the EGC temperature by means of eq. (4). More details on the computational procedure can be found in ref. [39]. Because of the lack of the thermodynamic excess properties of any phase, only excess Gibbs energy differences ($\Delta_\phi^\gamma G^E$) have been determined.

The description of the difference of the excess magnitudes has been done through a two temperature-independent parameter Redlich–Kister polynomial function:

$$\Delta_\phi^\gamma F^E(X) = X(1-X)\left[\Delta_\phi^\gamma F_1 + \Delta_\phi^\gamma F_2(1-2X)\right] \quad (5)$$

which in the lack of strong local anomalies is fairly adequate and physically understandable: $\Delta_\phi^\gamma F_1$ expresses the magnitude of the excess property difference at the equimolar composition and $\Delta_\phi^\gamma F_2$, gives account for the asymmetry of such a function with respect to X = 0.5.

[FCC+L] two-phase equilibria. As for the [FCC+L] equilibrium the evidence of the isomorphism relationship between the stable FCC phases of 1-BrA and 1-ClA as demonstrated by the continuity of the (*T*,*X*) loop as well as by the lattice cubic parameter (continuous formation of mixed crystals), thermodynamic assessment can be easily done

[**Fig. 4(b)**] by applying eq. (2) for ϕ = FCC and γ = L. The experimental temperature and enthalpy and entropy changes of the pure compounds can be found in **Table 1**.

Crossed isopolymorphism: [M+FCC], [O+FCC] and [M+O] two-phase equilibria. The crossed isopolymorphism concept entails for each phase of component A (or B) the existence of an isomorphous (stable or metastable) phase for compound B (or A). Thus, extension of the [M+O] and [O+FCC] loops at X = 1 and the [M+FCC] at X = 0 provide the metastable phase transitions M to O and O to FCC for 1-ClA and, similarly, from M to FCC for 1-BrA. These extrapolations concerning temperatures are indicated in **Fig. 4(a)**. Fortunately, the stable two-phase equilibria extend over the ca. 50% of the mole composition, so the extrapolation entails reasonable errors.

Assuming that heat capacity values for the different phases are close and owing to the closeness of the transition (stable or metastable) temperatures, the associated enthalpy changes (**Fig. 5**) can be combined by:

$$\Delta H_{M\rightarrow FCC} = \Delta H_{M\rightarrow O} + \Delta H_{O\rightarrow FCC} \quad (6)$$

which enables to expand experimental data and makes possible and physically coherent to extrapolate enthalpy changes for the metastable phase transitions. **Table 1** gathers experimental and extrapolated (italic) values for the phase transitions of pure compounds. **Figure 4** evidences the perfect agreement between experimental and calculated phase diagram (experimental temperature points may deviate from the mean trend to a maximum of about 1.5 K for the melting and [FCC+L] equilibrium while and no more than about 2 K for the equilibria involving the low-temperature phases), which in turns enhances the validity of the extrapolated phase transition properties of pure compounds.

The obtained excess Gibbs energy differences in the form of Redlich-Kister polynomial coefficients are compiled in **Table 3**.

Table 3.- $\Delta_{\phi}^{\gamma}F_1 = F_1^{\gamma} - F_1^{\phi}$ and $\Delta_{\phi}^{\gamma}F_2 = F_2^{\gamma} - F_2^{\phi}$ parameters of the Redlich-Kister polynomial (see eq. 5) for the excess Gibbs energy ($F \equiv G$) difference and for the excess Enthalpy ($F \equiv H$) difference between the involved phases in the 1-BrA+1-ClA two-component system together with the equimolar Equal-Gibbs temperature [T_{EGC} (X = 0.5)] for each of the assessed equilibria across the $\phi \rightarrow \gamma$ transition.

Equilibrium	ϕ	γ	$\Delta_{\phi}^{\gamma}G_1$ J mol^{-1}	$\Delta_{\phi}^{\gamma}G_2$ J mol^{-1}	T_{EGC} **(X = 0.5)** K
[FCC+L]	FCC	L	-203.1	76.1	411.4
[O+FCC]	O	FCC	488.6	-442.0	284.1
[M+FCC]	M	FCC	469.3	-442.0	
[M+O]	M	O	-19.3	0	
Equilibrium	ϕ	γ	$\Delta_{\phi}^{\gamma}H_1$ J mol^{-1}	$\Delta_{\phi}^{\gamma}H_2$ J mol^{-1}	

[FCC+L]	FCC	L	-1133.0	442.7
[O+FCC]	O	FCC	-2638.8	222.3
[M+FCC]	M	FCC	-1517.9	-1278.3

4. Discussion

The thermodynamic assessment enables us the knowledge of the excess (difference) properties of the involved phases. Excess thermodynamic functions for any phase of the mixtures 1-BrA+1-ClA are unknown. Thus, strictly only excess Gibbs energy and enthalpy differences between phases can be obtained.

For the 1-BrA+1-ClA system, whatever the ϕ and γ phases are involved, $\Delta^{\gamma}_{\phi}H_1$ are negative, which means that on going from the high-temperature liquid phase to FCC, O and the lowest-temperature phase M, the excess enthalpy always increases. This can be considered as the usual behavior, because the energy interactions produced by substituting a molecule of B into the liquid phase of A would be lower than into the OD FCC phase and much lower than in the orientationally ordered O and M phases [41-43]. As can be seen in **Fig. 9(a)**, the smallest excess enthalpy difference corresponds to the [FCC+L] equilibrium.

The excess energy $H^{E,\phi}$ reflects the energetic interaction between the molecules A and B of the two components. It will be zero if this interaction is neutral, i.e., the mean of the interaction between A and A and between B and B molecules. Instead, it will be negative if there is a net attraction between A and B molecules, and positive in the case of a net repulsion. If in our case we reasonably assume an ideal liquid mixture, i.e., $H^{E,L} = 0$, then the excess energy of the mixture will be positive for all solid phases, becoming larger as lower-temperature phases are reached ($H^{E,M} > H^{E,O} > H^{E,FCC}$). Hence, it would mean that there exists a repulsion between A and B components.

On the other hand, it should be mentioned here that concerning the two factors ruling the miscibility in the solid state, namely, the steric factor and the molecular symmetry factor, only the first one must be considered here owing to the fact of the identical molecular symmetry of the involved compounds, C_{3v}, as well as the same space group for the monoclinic and OD FCC phases and for the superimposed isostructural orthorhombic phase. Thus, the lattice parameters for the ordered monoclinic and OD FCC phases as a function of composition slightly deviate from the Vegard's law (see **Fig. 6**) and consequently mixed crystals are purely governed by steric effects.

The relatively large excess enthalpy difference for the [FCC+L] equilibrium is contrasting with the excess Gibbs energy difference, which is quite small. In fact, as can be seen in the top panel of **Fig. 4**, the [FCC+L] two-phase region bends only slightly downwards. It means that there is a small negative value of $\Delta^{L}_{FCC}G^{E}$ and subsequently, as $\Delta^{L}_{FCC}G^{E} = \Delta^{L}_{FCC}H^{E} - T\cdot\Delta^{L}_{FCC}S^{E}$, it follows that, according to the negative excess enthalpy difference $\Delta^{L}_{FCC}H^{E}$ depicted in **Fig. 9(a)**, the entropy factor $\Delta^{L}_{FCC}S^{E}$ contributing to the excess Gibbs energy difference, is greatly negative. In other words, a kind of order is provided for the OD mixed crystals with respect to the liquid state.

As far as the [M+FCC] and [O+FCC] mixed crystals, the excess enthalpy differences [see **Fig. 9(a)**] are quite negative, whereas the [M+FCC] and [O+FCC] two-phase regions (see **Fig. 4**) are slightly upward, as the positive excess Gibbs energy differences [**Fig. 9(b)**]

clearly show. Consequently, the entropic term of the excess Gibbs energy difference, $\Delta_{\alpha}^{FCC}G^{E} = H^{E,FCC} - T{\cdot}S^{E,\alpha}$ for α = M, O, for such equilibria must compensate by means of a large negative value, even larger than for the [FCC+L] equilibrium. This means that $T{\cdot}S^{E,FCC} < T{\cdot}S^{E,\alpha}$ for both α = M and α = O. Such an inequality should be attributed to the easiness of formation of mixed crystals into an orientationally disordered phase, as it was shown previously in many other two-component systems involving such phases [1-7].

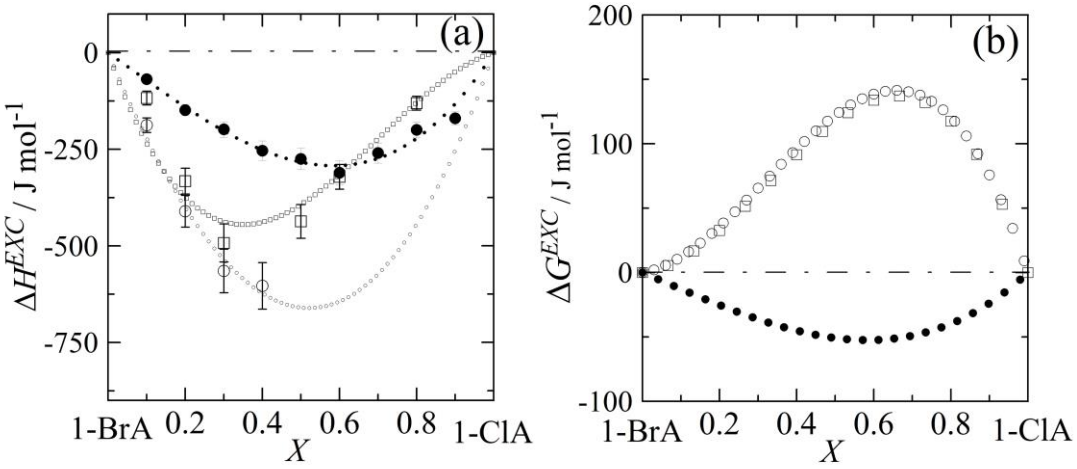

Fig. 9. Excess enthalpy differences, $\Delta_{\phi}^{\gamma}H^{E}(X) = H^{E,\gamma} - H^{E,\phi}$ (a) and excess Gibbs differences $\Delta_{\phi}^{\gamma}G^{E}(X) = G^{E,\gamma} - G^{E,\phi}$ (b), for the [M+FCC] (empty squares), [O+FCC] (empty circles) and [FCC+L] (full circles) equilibria at their Equal-Gibbs-Curve temperatures.

As we have demonstrated, despite of the similarity of the 1-BrA and 1-ClA molecules, the polymorphic behavior at normal pressure, i.e., in equilibrium with its vapor, is found to be quite different. In particular, the orthorhombic phase for the 1-ClA does not appear at normal pressure, thus being metastable (monotropic) with respect to both FCC and M phases. The question that emerges is if this orthorhombic phase has an overall monotropic behavior, i.e., if the metastable character remains whatever the pressure or if it behaves enantiotropically at high pressure, at least at pressures higher than those experimentally studied [0-300 MPa, see **Fig. 2(b)**]. To find out such stability relationships between the solid phases, the topological temperature-pressure (*P*-*T*) phase diagram must be calculated [44-50]. A topological *P*-*T* phase diagram accounts for the phase relationships between all the polymorphs and the vapor and liquid phases and it is a consequence of the basis of thermodynamics established by Gibbs. For such a task, two-phase equilibria in the *P*-*T* phase diagram can be represented by straight lines calculated through the Clapeyron equation:

$$\frac{dT}{dP} = \frac{\Delta v}{\Delta S} = \frac{T\Delta v}{\Delta H} \tag{7}$$

As for the case study here, due to the known stability domains of the monoclinic, at low-temperature, and the FCC, at high-temperature, phases, there are only two possibilities concerning the slopes of the solid-solid equilibria involving the M, O and FCC solid phases:

$$\left(\frac{dT}{dP}\right)^{O\to FCC} < \left(\frac{dT}{dP}\right)^{M\to FCC} < \left(\frac{dT}{dP}\right)^{M\to O} \tag{8a}$$

$$\left(\frac{dT}{dP}\right)^{M\to O} < \left(\frac{dT}{dP}\right)^{M\to FCC} < \left(\frac{dT}{dP}\right)^{O\to FCC} \tag{8b}$$

These two possible scenarios are represented in **Figs 10(a)** and **10(b)**, respectively.

To elucidate the complete polymorphic behavior of 1-ClA compound, we can make use of the thermodynamic properties derived from the two-phase equilibria (as transition temperatures and enthalpy changes) as well as by the volumes derived from X-ray diffraction by extrapolating as a function of the mole fraction to the pure compounds for which the involved transitions do not exist at normal pressure.

The transition temperatures and enthalpy changes have been derived from the thermodynamic assessment and they are gathered in **Table 1**. As for the volume changes, **Fig. 7** provides the volume of the metastable orthorhombic phase of 1-ClA from simple extrapolation. Assuming that the thermal expansion of this O phase would be similar to the O stable phase of 1-BrA, as it happens for the monoclinic phases of both compounds (see **Fig. 11** where molar volumes are represented as a function of temperature for both compounds), values of the metastable O phase for 1-ClA can be obtained [see **Fig. 11(b)**]. It should be mentioned here that owing to the narrow temperature range of the O phase, the assumption of virtually the same thermal expansion is irrelevant as far as the obtained volume changes for the O to FCC and M to O metastable transitions for 1-ClA.
According to the obtained molar volume for the O phase of 1-ClA, the volume changes $\Delta v^{M\to O}$ and $\Delta v^{O\to FCC}$ can be determined. They are represented in **Fig. 11(b)** and gathered in **Table 1**.

Once the thermodynamic data have been obtained, the subsequent step is tracing the equilibrium lines using the Clapeyron eq. (7). At the intersections of the equilibrium lines, the positions of the triple points can be found, which make up the framework of a topological *P-T* phase diagram. As can be seen from the obtained values for the calculated slopes in Table 1: $\left(\frac{dT}{dP}\right)^{O\to FCC} < \left(\frac{dT}{dP}\right)^{M\to FCC} < \left(\frac{dT}{dP}\right)^{M\to O}$**,** [i.e., (0.28±0.08) K MPa^{-1} < (0.33 ± 0.04) K MPa^{-1} < (0.71±0.21) K MPa^{-1}]. The high value of the slope $\left(\frac{dT}{dP}\right)^{M\to O}$, much beyond the error, makes clear that the topological phase diagram for 1-ClA corresponds without any doubt to that depicted in **Fig. 11(a)**, which indicates that the O phase of 1-ClA displays overall monotropy, i.e., it is metastable whatever the pressure, in agreement with the experimental phase diagram shown in **Fig. 2(b)**. As a consequence, the triple point

[M+O+FCC] between the three involved solid phases appears at negative pressures. That the O phase for 1-ClA appears as metastable whatever the pressure is, as established by Bridgman, a consequence of the larger volume of the metastable phase with respect to the M phase, in such a way that application of pressure will only increase the relative metastability of the metastable form [51].

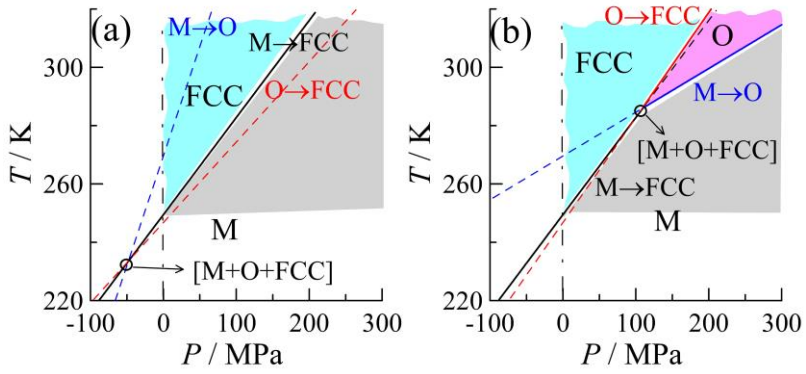

Fig. 10. Possible topological pressure-temperature phase diagrams of 1-ClA concerning the solid phases M, O and FCC for the overall monotropy of the O phase (a) and for the monotropic behavior of O phase at normal pressure and enantiotropic behavior at high pressure (b).

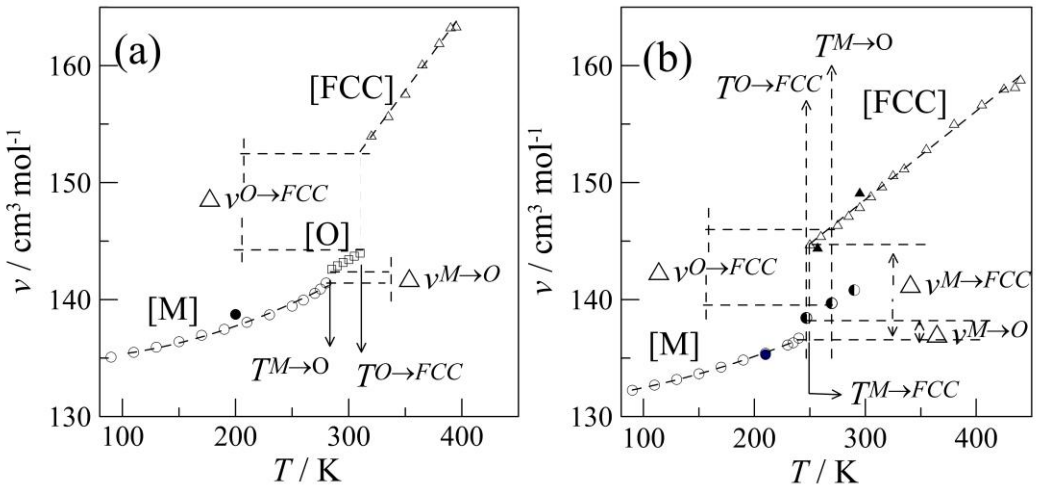

Fig. 11. Molar volume of 1-BrA (a) and 1-ClA (b) as a function of temperature derived from X-ray diffraction experiments for the solid phases. Filled symbols correspond to values previously published for the M [26] and FCC [27] phases of 1-BrA and for the M [25] and FCC [25] phases of 1-ClA. Half filled circles in (b) represent the extrapolated values from X-ray diffraction as a function of the mole fraction for the orthorhombic metastable phase of 1-ClA.

5. Conclusions

By combining different experimental techniques as well as basic thermodynamics, we have provided information not only about the stable experimentally available phases as a function of temperature and pressure but also on the non-experimentally available properties and transitions of metastable phases. In particular, we have accounted for the polymorphic behavior of 1-Br-adamantane and 1-Cl-adamantane from the low temperature monoclinic phase through the liquid state and as a function of pressure. Whatever the pressure, the phase sequence on increasing temperature for 1-Br-adamantane is found to be monoclinic, orthorhombic, face-centered cubic and liquid. As for 1-Cl-adamantane, the sequence is similar, with the exception of the orthorhombic phase, which does not appear. The two-component system [1-Br-adamantane+1-Cl-adamantane] here studied enables us, on the basis of the crossed isopolymorphism concept, a straightforward method to determine the metastable transition points and phase properties at normal pressure for non-experimentally available phases. These properties are used to infer the topological pressure-temperature phase diagram, which demonstrates that, for 1-Cl-adamantane, the orthorhombic phase displays overall monotropy, i.e., it is metastable with respect to the monoclinic and to the face-centered cubic phases whatever the pressure.

We have shown that the low-temperature monoclinic and the high-temperature orientationally disordered face-centered cubic phases of these 1-X-adamantane derivatives are isomorphous and form continuous series of mixed crystals, being both excess enthalpy differences $\Delta_{FCC}^{L}H^{E}$ and $\Delta_{M}^{FCC}H^{E}$ negative. The formation of orthorhombic mixed crystals for a noticeable domain of composition also indicates a negative excess enthalpy difference $\Delta_{O}^{FCC}H^{E}$. This negative sign for $\Delta_{\phi}^{\gamma}H^{E}$ in all cases entails that the excess enthalpy H^{E} always increases when going to a lower-temperature phase. Assuming an ideal behavior for the liquid phase results in positive excess energy H^{E} for all kind of mixed crystals, which means that there is a net repulsion between the molecular entities A and B with respect to the ideal mixture.

Acknowledgements

This work was supported by the Spanish Ministry of Economy and Competitivity (MEC) under project FIS2014-54734P and by the Catalan government (AGAUR) by the grant 2014SGR-581.

Appendix A. Supplementary data

Supplementary data associated with this article can be found, in the online version, at...

References

[1] L.C. Pardo, M. Barrio, J.-Ll. Tamarit, D.O. López, J. Salud, H.A.J. Oonk, Orientationally disordered mixed crystals sharing methylchloromethanes [$(CH_3)_{4-n}CCl_n$, n = 0, ..., 4], Chem. Mater. 17 (2005) 6146-6153.

[2] L.C. Pardo, B. Parat, M. Barrio, J.-Ll. Tamarit, D.O. López, J. Salud, Ph. Negrier, D. Mondieig, Non-experimentally available thermodynamic properties: The two-component system $(CH_3)CCl_3$+$CBrCl_3$, Chem. Phys. Lett. 402 (2005) 408-413.

[3] M. Barrio, L.C. Pardo, J.-Ll. Tamarit, Ph. Negrier, D.O. López, J. Salud, D. Mondieig, The two-component system CCl_4+$CBrCl_3$- inference of the lattice symmetry of phase II of $CBrCl_3$, J. Phys. Chem. B 108 (2004) 11089-11096.

[4] L.C. Pardo, M. Barrio, J.-Ll. Tamarit, J. Salud, D.O. López, Ph. Negrier, D. Mondieig, Multiple melting orientationally disordered mixed crystals of the two-component system $(CH_3)_2CCl_2$-$(CH_3)CCl_3$, Phys. Chem. Chem. Phys. 6 (2004) 417-423.

[5] L.C. Pardo, M. Barrio, J.-Ll. Tamarit, D.O. López, J. Salud, Ph. Negrier, D. Mondieig,Stable and metastable mixed crystals in the disordered state of the $(CH_3)CCl$-$(CH_3)_2CCl_2$ system, Chem. Phys. Lett. 355 (2002) 339-346.

[6] L.C. Pardo, M. Barrio, J.-Ll. Tamarit, D.O. López, J. Salud, Ph. Negrier, D. Mondieig, First experimental demonstration of the crossed isodimorphism: $(CH_3)_3CCl$+CCl_4 Phys. Chem. Chem. Phys. 3 (2001) 2644-2649.

[7] L.C. Pardo, M. Barrio, J.-Ll. Tamarit, D.O. López, J. Salud, Ph. Negrier, D. Mondieig, Stable and Metastable Phase Diagram of the Two-Component System $(CH_3)_3CCl$-$(CH_3)CCl_3$: An Example of Crossed Isodimorphism, J. Phys. Chem. B 105 (2001) 10326-10334.

[8] L.C. Pardo, M. Barrio, J.-Ll. Tamarit, D.O. López, J. Salud, Ph. Negrier, D. Mondieig, Miscibility study in stable and metastable orientational disordered phases in a two-component system $(CH_3)CCl_3$+CCl_4, Chem. Phys. Lett. 308 (1999) 204-210.

[9] D.O. López, J. Salud, M. Barrio, J.-Ll. Tamarit, H.A.J. Oonk, Uniform thermodynamic description of the orientationally disordered mixed crystals of a group of neopentane derivatives, Chem. Mater. 12 (2000) 1108-1114.

[10] M. Barrio, L.C. Pardo, J.-Ll. Tamarit, Ph. Negrier, D.O. López, J. Salud, D. Mondieig, Two-component system CCl_4 + $(CH_3)_3CBr$: Extrema in equilibria involving orientationally disordered phases, J. Phys. Chem. B 110 (2006) 12096-12103.

[11] M. Barrio, Ph. Negrier, L.C. Pardo, J.-Ll. Tamarit, D. Mondieig, Multiple crossed isopolymorphism: Two-component systems CCl_4+CBr_2Cl_2 and $CBrCl_3$+CBr_2Cl_2. Inference of metastable rhombohedral phase of CBr_2Cl_2, J. Phys. Chem. B 111 (2007) 8899-8909.

[12] J.-Ll. Tamarit, M. Barrio, L.C. Pardo, Ph. Negrier, D. Mondieg, High-pressure properties inferred from normal-pressure properties, J. Phys. Cond. Matter 20 (2008) 244110.

[13] R. Levit, M. Barrio, N. Veglio, J.-Ll. Tamarit, Ph. Negrier, L.C. Pardo, J. Sanchez-Marcos and D. Mondieig, From the two-component system $CBrCl_3$ + CBr_4 to the high-pressure properties of CBr_4, J. Phys. Chem. B 112 (2008) 13916-13922.

[14] M. Barrio, J.-Ll. Tamarit, R. Céolin, L.C. Pardo, Ph. Negrier, D. Mondieig, Connecting the normal pressure equilibria of the two-component system $CCl(CH_3)_3$ +$CBrCl_3$ to the pressure-temperature phase diagrams of pure components, Chem. Phys. 358 (2009) 156-160.

[15] M. Barrio, Ph. Negrier, J.-Ll. Tamarit, D. Mondieig, From high-temperature orientationally disordered mixed crystals to low-temperature complexes formation in the two-component system $(CH_3)_3CBr$+ Cl_3CBr J. Phys. Chem. B 115 (2011) 1679-1688

[16] P. Espeau, R. Céolin, Thermodynamic studies of solids with non-negligible vapor pressure: *T*-*v* and *p*-*T* diagrams of the dimorphism of adamantane, Thermochim. Acta 376 (2001) 147-154 and references therein.

[17] M. Romanini, Ph. Negrier, J.-Ll. Tamarit, S. Capaccioli, M. Barrio, L.C. Pardo, D. Mondieig, Emergence of glassy-like dynamics in an orientationally ordered phase, Phys. Rev. B 85 (2012) 134201.

[18] Ph. Negrier, M. Barrio, M. Romanini, J.-Ll. Tamarit, D. Mondieig, A.I. Krivchikov, L. Kepinski, A. Jezowski, D. Szewczyk, Polymorphism of 2-Adamantanone, Cryst. Growth Des. 14 (2014) 2626-2632.

[19] B. Ben Hassine, Ph. Negrier, M. Barrio, D. Mondieig, S. Massip, J.-Ll. Tamarit, Phase transition in hydrogen-bonded 1-adamantane-methanol, Cryst. Growth Des. 15 (2015) 4149−4155.

[20] D. Szewczyk, A. Jezowski G.A.Vdovichenko, A.I. Krivchikov, F.J. Bermejo, J.-Ll. Tamarit, L.C. Pardo, J.W. Taylor, Glassy dynamics versus thermodynamics: The case of 2-adamantanone, J. Phys. Chem. B 119 (2015) 8468-8474.

[21] A.I. Krivchikov, G.A. Vdovichenko, O.A. Korolyuk, F.J. Bermejo, L.C. Pardo, J.-Ll. Tamarit, A. Jezowski, D. Szewczyk, Effects of site-occupation disorder on the low-temperature thermal conductivity of molecular crystals, J. Non-Cryst. Solids 407 (2015) 141-148.

[22] B. Ben Hassine, Ph. Negrier, M. Romanini, M. Barrio, R. Macovez, A. Kallel, D. Mondieig, J.-Ll. Tamarit, Structure and reorientational dynamics of 1-F-adamantane, Phys. Chem. Chem. Phys. 18 (2016) 10924-10930.

[23] M. Romanini, J.-Ll. Tamarit, L.C. Pardo, F.J. Bermejo, R. Fernandez-Perea, F.L. Pratt, Implanted muon spin spectroscopy on 2-O-adamantane: A model system that mimics the liquid→glass like transitions, J. Phys. Cond. Matter 29 (2017) 085405.

[24] L. Yuan, S. Clevers, A. Burel, Ph. Negrier, M. Barrio, B. Ben Hassine, D. Mondieig, V. Dupray, J.-Ll. Tamarit, G. Coquerel, A new intermediate polymorph of 1-fluoro-adamantane and its second-order like transition towards the low temperature, Cryst. Growth Des., in press (2017).

[25] M. Foulon, T. Belgrand, C. Gors, M. More, Structural phase transition in 1-chloroadamantane ($C_{10}H_{15}Cl$), Acta Cryst. B45 (1989) 404-411.

[26] R. Betz, P. Klüfers, P. Mayer, 1-Bromoadamantane, Acta Cryst. E65 (2009) o101.

[27] P. Zielinski, M. Foulon, Dynamics of Molecular Crystals, ed. by J. Lascombe, Elsevier Science Publisher, Amsterdam, 1987, p. 201-202.

[28] J.P. Amoureux, M. Bée, J.L. Sauvajol, Crystal structure of 1-chloroadamantane, $C_{10}H_{15}Cl$, in its plastic phase, Molec. Phys. 45 (1982) 709-719.

[29] Ph. Negrier, M. Barrio, J.-Ll. Tamarit, D. Mondieig, Polymorphism in 2-X-Adamantane Derivatives (X = Cl, Br), J. Phys. Chem. B 118 (2014) 9595-9603.

[30] A.B. Bazyleva, A.V. Blokhin, G.J. Kabo, A.G. Kabo, Y.U. Paulechka, Thermodynamic properties of 1-bromoadamantane in the condensed state and molecular disorder in its crystals, J. Chem. Thermodyn. 37 (2005) 643-657.

[31] K. Kobashi, T. Kyomen, M. Oguni, Construction of an adiabatic calorimeter in the temperature range between 13 and 505 K, and thermodynamic study of 1-chloroadamantane, Phys. Chem. Solids 59 (1998) 667-677.

[32] T. Clark, T.Mc.O. Knox, H. Mackle, M.A. McKervey, Order-disorder transitions in substituted adamantanes, J. Chem. Soc. Faraday Trans. 1 73 (1977) 1224-1231.

[33] A. Würflinger, Differential thermal-analysis under high-pressure IV. Low-temperature DTA of solid-solid and solid-liquid transitions of several hydrocarbons up to 3 kbar, Ber. Bunsen-Ges Phys. Chem. 79 (1975) 1195-1201.

[34] J. Ballon, V. Comparat, J. Pouxe, The blade chamber: A solution for curved gaseous detectors, Nucl. Instrum. Methods, 217 (1983) 213-216.

[35] MS Modeling (Materials Studio), version 5.5. http://www.accelrys.com.

[36] J.-Ll. Tamarit, I.B. Rietveld, M. Barrio, R. Céolin, The relationship between orientational disorder and pressure: The case study of succinonitrile, J. Mol. Struct. 1078 (2014) 3-9.

[37] J. Reuter, D. Büsing, J.-Ll. Tamarit, A.Würflinger, High-pressure differential thermal analysis study of the phase behaviour in sometert-butyl compounds: pivalic acid, 2-methylpropane-2-thiol and tert-butylamine, J. Mater. Chem. 7 (1997) 41-46.

[38] A. Aznar, P. Lloveras, M. Barrio, J.-Ll. Tamarit, Melting of orientational degrees of freedom, Eur. Phys. J. Special Topics 226 (2017) 1017–1029.

[39] H.A.J. Oonk, J.-Ll. Tamarit, Measurement of Thermodynamic Properties of Multiple Phases, in: R.D. Weir and T.W. de Loos (Eds), Experimental Thermodynamics, Volume VII, Ch.9, (IUPAC) Elsevier, Amsterdam, 2005.

[40] M.H.G. Jacobs, H.A.J. Oonk, *LIQFIT*. A computer program for the Thermodynamic Assessment of T-X liquidus or solidus data. Utrecht University (1990).

[41] M. Barrio, D.O. López, J.-Ll. Tamarit, Ph. Negrier, Y. Haget, Molecular interactions and packing in molecular alloys between nonisomorphous plastic phases, J. Solid State Chem. 124 (1996) 29-38.

[42] J. Salud, D.O. López, M. Barrio, J.-Ll. Tamarit, Two-component systems of isomorphous orientationally disordered crystals. Part 1 Packing of the mixed crystals, J. Mater. Chem. 9 (1999) 909-916.

[43] J. Salud, D.O. López, M. Barrio, J.-Ll. Tamarit, H.A.J. Oonk, Two-component systems of isomorphous orientationally disordered crystals. Part 2 Thermodynamic analysis, J. Mater. Chem. 9 (1999) 917-922.

[44] M. Barrio, P. Espeau, J.-Ll. Tamarit, N. Veglio, R. Céolin, Polymorphism of progesterone: relative stabilities of the orthorhombic phases I and II inferred from topological and experimental pressure-temperature phase diagrams, J. Pharm. Sci., 98 (2009) 1657-1670.

[45] M. Barrio, P. de Oliveira, R. Céolin, D.O. López, J.-Ll.Tamarit, Polymorphism of 2-Methyl-2-chloropropane and 2,2-Dimethylpropane (Neopentane): Thermodynamic evidence for a high-pressure orientationally disordered rhombohedral phase through topological *p-T* diagrams, Chem. Mater. 14 (2002) 851-857.

[46] Ph. Espeau, R. Céolin, J.-Ll. Tamarit, M.A. Perrin, J.-P. Gauchi, F. Leveiller, Polymorphism of paracetamol: Relative stabilities of the monoclinic and orthorhombic phases inferred from topological pressure-temperature and temperature volume diagrams, J. Pharm. Sci. 94 (2005) 524-539.

[47] R. Céolin, J.-Ll. Tamarit, M. Barrio, D.O. López, B. Nicolaï, N. Veglio, M.-A. Perrin, Overall monotropic behavior of a metastable phase of Biclotymol, 2,2'-Methylenebis(4-Chloro-3-Methyl-Isopropylphenol), inferred from experimental and topological construction of the related *p-T* state diagram, J. Pharm. Sci. 97 (2008) 3927-3941.

[48] I.B. Rietveld, M. Barrio, Ph. Espeau, J.-Ll. Tamarit, R. Céolin, Topological and experimental approach to the pressure-temperature-composition phase diagram of the binary enantiomer system *d*- and *l*-Camphor, J. Phys. Chem. B 115 (2011) 1672-1678.

[49] I. Gana, M. Barrio, B. Do, J.-Ll. Tamarit, R. Céolin, I.B. Rietveld, Benzocaine polumorphism: Pressure-temperature phase diagram involving forms II and III, Int. J. Pharm. 456 (2013) 480-488.

[50] M.-A. Perrin, M. Bauer, M. Barrio, J.-Ll. Tamarit, R. Céolin, I.B. Rietveld, Rimonabant dimorphism and its pressure-temperature phase diagram: A delicate case of overall monotropic behavior, J. Pharm. Sci. 102 (2013) 2311-2321.

[51] P.W. Bridgman, The physics of high pressure, Dover, New York, 1970.